

# Structural health monitoring of slab-column connections using FBG sensors

E. Rizk · H. Marzouk ·  
A. Hussein · X. Gu

Received: 12 June 2011 / Accepted: 20 December 2011 / Published online: 19 January 2012  
© Springer-Verlag 2012

**Abstract** Health monitoring of reinforced concrete structures is a very important technique to maintain structural integrity. Early detection of damage can save lives and costly repairs. The information obtained from monitoring is generally used to plan and design maintenance activities, increase the safety, verify hypotheses, and reduce uncertainty. The current research is focused on the development and optimization of a structural health monitoring concept to detect damage initiation for slab-column connections. The research objective is to detect, localize and quantify flexural (service) cracks and shear cracks in slab-column connections. The experimental program is divided into three phases. The first phase is focused on detection of flexural cracks using embedded fibre Bragg grating (FBG) sensors. Detection of flexural cracks includes the initiation of first crack as well as the initial crack width. The second phase is focused on mapping of crack patterns using FBG sensors arrays. The last phase of the experimental work includes detection and localization of shear cracks as well as quantification of high compressive (bearing) zones using three-dimensional configuration

of FBG sensor arrays. The current research presents the first phase of the experimental work. Test results revealed that embedded FBG sensors exhibited excellent performance and it was able to monitor the width and location of the first crack.

**Keywords** Flexural cracks · Shear strains · Shear cracks · Punching · Structural health monitoring · Long FBG · Array

## 1 Introduction

The two-way slab system is a unique efficient structural system. It is economical and is widely used in different structural applications such as floors, roofs of buildings and walls of tanks. The two-way slab system is also used as a structural component in concrete offshore platforms and nuclear containment structures. A major concern of this system is localized punching shear failure at the slab-column connection. The catastrophic nature of punching shear failure has been a major concern for engineers for many years. Detecting cracks and local damages as early as possible is one of the most essential functions of a successful SHM system for a slab-column connection. Most of the previous research on SHM was carried out on one-dimensional elements such as beams. SHM of two-way slabs used for offshore construction is critical and is not fully addressed.

The current research presents different SHM techniques to detect, localize and quantify damage in two-way slab system. The experimental work is divided into three main phases. The first phase is focused on detection of the initiation of service cracks using embedded fibre Bragg grating (FBG) sensors. The second phase is focused on

---

E. Rizk (✉) · A. Hussein  
Faculty of Engineering and Applied Science,  
Memorial University of Newfoundland,  
St. John's, NF A1B 3X5, Canada  
e-mail: emad.rizk@mun.ca

H. Marzouk  
Department of Civil Engineering,  
Faculty of Engineering, Architecture and Science,  
Ryerson University, Toronto, ON M5B 2K3, Canada

X. Gu  
Department of Electrical and Computer Engineering,  
Faculty of Engineering, Architecture and Science,  
Ryerson University, Toronto, ON M5B 2K3, Canada

mapping of service cracks patterns using bonded FBG sensors arrays. The technique combines two main capabilities of FBG sensors. The first capability is the ability of long FBG sensors to detect initiation of cracks. The second capability reflects the advantage of multiplexing several FBG sensors onto the same optical fibre. The last phase of the experimental work includes detection and localization of punching shear cracks as well as quantification of high compressive (bearing) zones using three-dimensional configuration of FBG sensors array. This paper presents the results of the first phase of the experimental work. In this work, embedded FBG sensors were applied for health monitoring of two-way concrete slab. The main objective of the experimental work is to develop a SHM technique for offshore concrete structures that enables continuous health monitoring of the structure as well as the capability to detect the width and location of first crack. Two sets of FBG and electrical strain gauge (ESG) sensors were mounted on tensile rebars. The FBG sensor is bonded onto a flattened surface at the middle of a reinforcement rebar. A different type of long FBG sensor is embedded in the tension side of the concrete slab.

## 2 Structural health monitoring (SHM) and damage detection

Structural health monitoring is defined as the process of implementing a damage detection strategy for aerospace, civil, and mechanical engineering infrastructure. It consists of permanent continuous, periodic or periodically continuous recording of representative parameters, over short or long terms. Although sometimes SHM refers to damage detection, it could be used to refer to the process of quality assurance of the properties of new structures, long-term monitoring of an existing structure, structural control and many others. In the most general terms, damage can be defined as changes introduced into a system that adversely affects its current or future performance. Implicit in this definition is the concept that damage is not meaningful without a comparison between two different states of the system, one of which is assumed to represent the initial and often undamaged state. Identifying the presence of the damage might be considered as the first step to take preventive actions and to start the process towards understanding the root causes of the problem. A widely accepted definition of the levels of damage detection was provided [1]. The researcher defined four levels of damage identification: detection of the damage, localization of the damage, quantification of damage and decision-making.

In general, monitoring can be performed at the local material level or at the structural level. Monitoring at the material level provides information related to the local

material behaviour, but gives reduced information concerning the behaviour of the structure as a whole. Monitoring at the structural level provides better information related to the global structural behaviour and indirectly, through the changes in structural behaviour, also provides information related to material performance. To perform monitoring at a structural level, it is necessary to cover the structure, or a part of it, with sensors.

## 3 Optical FBG sensors

Fibre Bragg grating sensors are one of the many fibre optic sensor technologies that are currently being used in SHM systems. The sensors operate by detecting a shift in the wavelength of the reflected maximum due to applied strain. FBG sensors have been studied for a wide variety of mechanical sensing applications [2–5] including monitoring of civil infrastructures (highways, bridges, buildings, dams, etc.). The main advantage of FBGs for mechanical sensing is that these devices perform a direct transformation of the sensed parameter to optical wavelength, independent of light levels, connector or fibre losses, or other FBGs at different wavelengths.

Test results revealed that the gauge length of FBG sensors should be at least two or three times longer than the size of the coarse aggregate, in order to get a good averaged value [6]. Most FBGs and associated instrumentation are manufactured at an operating Bragg wavelength of 1,530–1,550 nm. FBGs are not electrically conductive and thus can be employed in hostile environments where electrical currents might pose a hazard.

One of the conditions of FBG that has to be made clear before using it is that the sensors cannot measure two different parameters at the same time and position. Since the wavelength of a FBG shifts with temperature and strain, in real environments and on real structures, both of these will be varying. However, there is a requirement that one is measured independently of the other. One technique for measuring only one parameter is to null the other. For example, if a strain measurement is required, then a dummy FBG shall measure the effect of temperature at the same position [7].

### 3.1 Sensor gauge length and measurement

Optical-fibre sensors can be classified according to its gauge length into short-gauge and long-gauge sensors. Traditional sensors, such as strain gauges and vibrating wires, belong to the group of short-gauge sensors. The development of long-gauge fibre optic sensors has opened new and interesting possibilities for structural monitoring. Long-gauge sensors allow the measurement of deformations over measurement

bases that can reach tens of metres with resolutions in the micrometer range. Using long-gauge sensors allow the monitoring of a structure as a whole, so that any phenomenon that has an impact on the global structural behaviour is detected and quantified. This constitutes a fundamental departure from standard practice that is based on the choice of a reduced number of points supposed to be representative of the whole structural behaviour and their instrumentation with short-gauge sensors.

A long-gauge deformation sensor is by definition a sensor with a gauge length several times longer than the maximum distance between discontinuities in a monitored material. For example, in the case of cracked reinforced concrete, the gauge length of a long-gauge sensor is to be several times longer than the maximum distance between cracks [8]. The main advantage of this measurement is in its nature; since it is obtained by averaging the strain over long measurement basis, it is not influenced by local material discontinuities. Thus, the measurement contains information related to global structural behaviour rather than the local material behaviour.

### 3.2 Sensor embedment issues in concrete

One of the key features of optical fibres is geometric conformity and capability for embedment within materials during their production such as in fresh concrete. Fragility of optical fibres, however, has been a hindrance to rapid employment of the technology in infrastructure projects. Issues involved include design of relevant protective gear for the optical fibre without jeopardizing sensing capability, durability within the concrete and surviving the harsh construction environment. Depending on the desired location, the long FBG sensor is either positioned in place by the seats used for positioning of the reinforcement within the depth of the structural member or can be tied across the rebars. One of the main disadvantages of long FBG sensors when embedded in concrete is their susceptibility to fragile. In the current paper, to guard against damage during concrete placement and handling, long FBG sensors were protected with stainless steel tubes.

## 4 Detection of cracks using FBG sensors

Embedded FBG sensors have been used successfully by many researchers to detect and locate cracks. Uncoated FBG sensors embedded in CFRP cross-ply laminates were applied for the detection of transverse cracks [9]. The researchers found that the uncoated optical fibres have problems in handling for embedding, and the durability of the fibres is lower than that of coated optical fibres. FBG sensors were successfully multiplexed in a series along a

signal fibre, and were embedded in or surface mounted onto a prestressed concrete beam to measure strain and temperature during curing and prestress conditions [10]. The suitable placement of a network of FBG sensors allowed the researchers to detect the location and depth of cracks when the beam was subjected to heavy loading.

Ansari [7] presented an example of a long-gauge sensor specifically designed for monitoring the deformations and cracks in reinforced concrete bridge decks. The sensor consists of a 3-mm diameter threaded rod and a shear key at each end. The threaded rod is made of stainless steel and a groove that runs along the 1,000 mm gage length of the rod to a depth of 1.5 mm. The optical fibre is inserted within the groove and sealed in place with a water resistant epoxy. The reflective ends of the optical fibre are extended through the shear keys and are protected in the brass tubes adjacent to the shear keys. Optical fibres from the adjacent sensors run through the brass tube and link through ferrules. This particular sensor was designed to detect cracking and therefore was not made to adhere to the reinforcement.

Silva-Munoz and Lopez-Anido [11] used distributed embedded FBG sensors located at different layers of a composite joint for damage monitoring of composite joints based on strain measurements using embedded FBG sensors. The researchers found that embedment of multiple FBG sensors was able to detect changes in strain due to crack extension during fatigue loading. Takeda et al. [12] developed an innovative crack detection technique using two FBG sensors embedded at both edges of a crack arrester. The researchers were able to detect the crack propagation in a double cantilever beam by comparing these two reflection spectra.

Based on previous review, it was noted that different researchers [9–12] listed different interpretations to explain crack detection that include spectral shape, shift, and effects of testing to the reflected spectra. However, the clearest indication of crack initiation was noticed by a sudden increase in the wavelength magnitude [7, 8], and this was the consequence of crack formation that allowed the detection of damage (cracking). In the current research, the crack formation was detected by monitoring the concrete tensile strain versus time. The initiation of cracks was detected by a sudden shift in the wavelength magnitude. Hence, if it is required to apply FBG sensors for crack detection of full-scale structures, the FBG sensors should be embedded/bonded at the points where cracks are expected to occur earlier than other points. If transverse cracks occur, the reflected spectrum is distorted, and the strain determined from wavelength shift does not strictly agree with average strain. Hence, this wavelength shift represents a crack opening. This means that long FBG sensors could be applied successfully to detect the

initiation of cracks. In order to obtain the accurate locations of sensor's monitoring points, a rational strut-and-tie model (STM) could be applied. The following sections present different strategies to obtain optimum locations of health monitoring sensors for concrete plate members.

## 5 Health monitoring of slab-column connection

A two-way slab is a structural element subject to biaxial bending, torsional moment, as well as membrane and shear forces. Structural monitoring of two-way slab element poses some challenges that require careful selection of effective sensors locations or a large number of sensors will be required for slab monitoring, which can be very costly. In order to reduce the monitoring costs, it is recommended to monitor only the critical damage zones in the slab. In order to minimize the number of sensors used, a STM could be applied to obtain the optimum number of sensors as well as the accurate sensor locations.

### 5.1 Damage locations in slab-column connections

Figure 1 shows the general punching idealization of the shear behaviour of a uniformly loaded plate supported by a column. The inclined shear crack that develops from the top surface at an angle  $\theta$ , and forming the critical section is shown. Damage could be detected in slab-column connections in three possible zones, as shown in Fig. 1. The first zone contains flexural (service) cracks that form in the tensile zone of the plate and have a wedge shape, with the maximum crack width at the tension face and zero width near the neutral plane. Flexural cracks begin to occur when concrete stress in the tension face of the plate reaches the tensile strength of concrete. Crack control is an important serviceability limit state. The second zone is the shear cracking zone. Cracking in this zone is dependent on the diagonal tensile strength of the concrete. In general, the inclined shear crack forms at a load level of 60–90% of the ultimate punching load. These cracks form at the critical

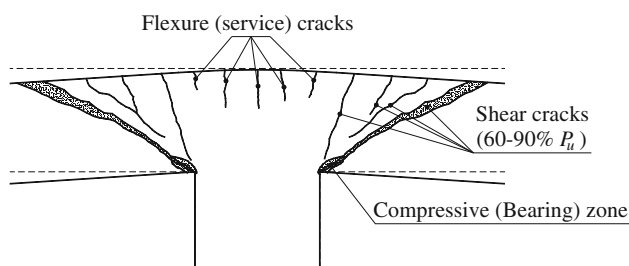


**Fig. 1** Punching failure mechanism of a concrete plate

section and completely surround the punching load area. The plate at this level can be unloaded and reloaded without any decrease in the ultimate punching capacity. Although ultimate punching shear failure of the plate is not dependent on the shear crack zone, this zone is important in that the presence of cracking in this zone around the periphery of the punching load area may be a warning sign, that the applied loads are nearing the ultimate punching shear level. In many structures, such as flat plate structures, the presence of punching shear cracks is to be avoided and knowledge of the cracking mechanism behaviour is required. One of the major challenges in damage detection of concrete structures is the capability to detect shear cracks that are very unpredictable. The third zone is the compressive (bearing) zone that exists at the loading area (column head). This zone extends from the plate neutral plane to the compression face of the plate. This zone is where the ultimate punching shear capacity of the plate is governed. Punching of the plate occurs when the concrete in this zone fails by a high concrete compression stress. This zone will be termed the ultimate failure zone. The zones in Fig. 1 are shown in two-dimensional for simplicity; however, they are actually three-dimensional “cone-shaped” fields located around the perimeter of the loading area.

### 5.2 Flow of forces in concrete plates

The complex internal flow of forces in a plate can be modelled using rational and simple STM. The STM considers the flow of forces within a structural element to consist of a series of compressive struts and tension ties joined at nodes. In this model, cracked concrete carries loads through sets of compressive fields that are distributed and interconnected by tension ties. The tension ties are reinforcing bars or concrete tensile stress fields. Muttoni and Schwartz [13] assumed that the shear strength of concrete plates is reduced by the presence of a critical shear crack that propagates through the plate into an inclined compression strut carrying the shear force to the load (Fig. 2a). A STM was recommended [14] to evaluate the punching shear capacity of concrete plates. Marzouk et al. [15] proposed an enhanced STM to evaluate the punching shear capacity of thick plates. The STM for symmetric punching consists of a “bottle-shaped” strut in the tension zone of the plate leading to a “rectangular-shaped” strut in the compressive zone. Inclined shear cracking develops in the bottle-shaped strut prior to failure in the compressive zone. Cracking in the bottle-shaped strut is related to the splitting tensile strength of the concrete. Ultimate punching failure occurs in the rectangular-stress zone by a high radial compressive stress failure (Fig. 2b).

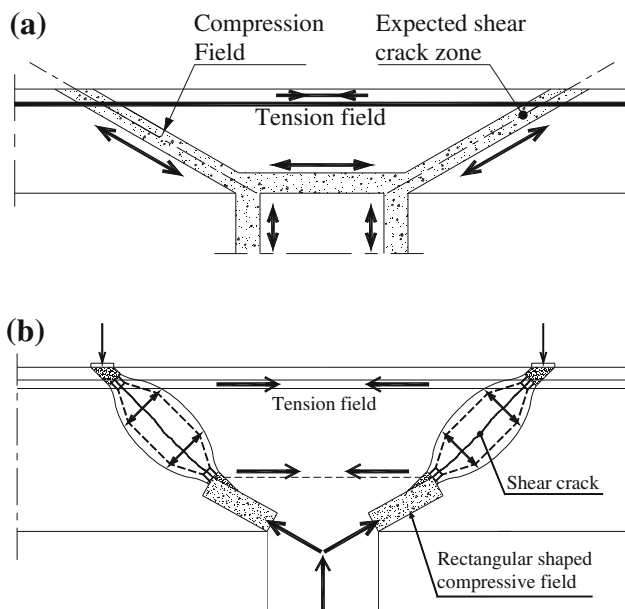


**Fig. 2** Flow of forces in a concrete plate: **a** thin plate, **b** thick plate

### 5.3 Cracking in plates and two-way slabs

Many researchers investigated the problem of cracking in plates and two-way slabs. Nawy and co-workers [16–18] tested over 90 two-way slabs. Test results revealed that flexural cracks were generated in two orthogonal directions as an image of the reinforcement when the spacing of intersections of the bars or wires, termed the grid nodal points, was such that the nodal points spacing did not exceed approximately 300 mm. Hossin and Marzouk [19] tested eight square full-scale specimens to investigate the crack width and spacing of high strength concrete (HSC) slabs used for offshore structures.

Rizk and Marzouk [20] investigated the cracking behaviour of concrete plates. A special focus was given to thick concrete plates used for offshore and nuclear containment structures. Eight full-scale two-way slabs were designed and tested to examine the effects of concrete cover and bar spacing of normal and HSC on crack spacing. Crack width was measured using crack displacement transducers (CDT) that were mounted on the concrete surface of visible cracks, in order to measure the crack opening displacement. The results of the experimental work showed that for bar spacing of 300 mm and less, the flexural cracks developed in two orthogonal directions as a reflection of the reinforcement grid. Therefore, to control cracking in two-way slabs, the reinforcement spacing in two perpendicular directions is the major parameter to be considered. For test specimens with bar spacing greater than 300 mm, it can be speculated that the crack spacing behaves randomly. In that case, the dominant crack pattern is the radial crack pattern. Research work by Frosch [21]

that was implemented later in the recent ACI 318-05 code [22] abandoned the concept of crack width calculations to control crack through bar spacing limitation.

Based on the previous discussion, design guidelines could be established to help design engineers in selecting length and location of long FBG sensors in order to monitor flexural cracks' initiation in concrete plates or two-way slabs. From previous research work, for concrete plates with bar spacing less than 300 mm, it can be concluded that reinforcement rebars behave as crack initiators. Hence, the first possible crack location is expected to form above the bar that located at the middle of bending region. In order to make sure that the FBG sensor will intercept the crack path, it is recommended that the length of the sensor should be taken equal to  $1.0\text{--}2.0 s$ , where  $s$  is the bar spacing. The FBG sensor should be installed so that the sensor will cover at least two rebars.

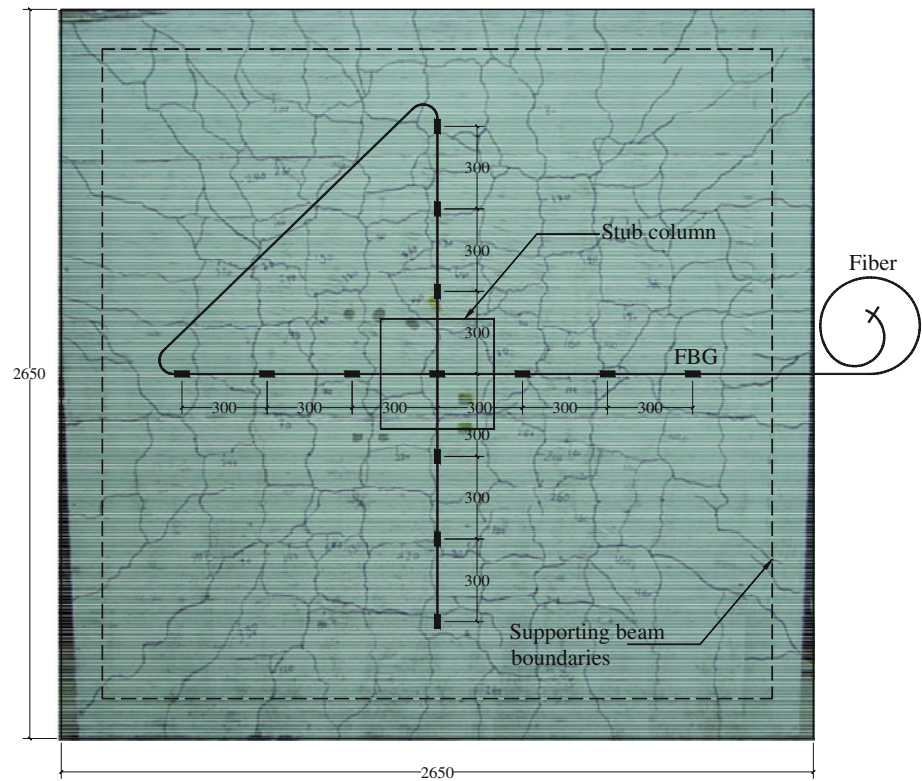
## 6 SHM of service and shear cracks

The first step in SHM process of two-way concrete slabs is to detect the location of first crack. The initiation of first crack is considered as the first warning sign that the concrete stresses reached the tensile strength of concrete. If the load is increased, new cracks form that result in reducing the spacing of cracks up to a certain limit “stabilized cracking stage”. In that case, crack formation stage is ended and no new cracks occur, but existing cracks widen. Long FBG sensors can be used to monitor the formation of first crack; this could be observed by a sudden increase in the strain magnitude. The sudden increase in strain could be converted into crack width by multiplying the strain by the sensor gauge length. The second step in SHM process is to localize and map crack patterns. Crack patterns for slabs provide insight into the failure mechanism and the rate of deterioration under loading. The prediction of crack patterns of a concrete slab, however, is a difficult problem. Crack patterns could be obtained using FBG sensors arrays. A less accurate but acceptable crack mapping could be obtained by assuming the crack to develop in a direction perpendicular to the FBG sensor array orientation (Fig. 3). For the slabs having high reinforcement ratio that failing by punching, the first radial cracks were found to be more pronounced along the lines parallel to the reinforcement passing through the column stub. Orthogonal cracking was the most dominant crack pattern [20].

In that case, it is recommended to arrange FBG sensors in the same manner as steel reinforcement. The main interesting advantage in using Bragg gratings resides in their multiplexing potential. Many gratings can be written in the same fibre at different locations and tuned to reflect at different wavelengths. This allows the measurement of



**Fig. 3** Crack pattern and schematic of FBG sensors arrays to map cracks



strain at different places along a fibre using a single cable, as shown in Fig. 3. Typically, 4–16 gratings can be measured on a single fibre line. In that case, it is recommended that the maximum grating length is less than or equal to 50 mm to achieve best results. However, this issue needs further investigation. It has to be noted that, since the gratings have to share the spectrum of the source used to illuminate them, there is a trade-off between the number of gratings and the dynamic range of the measurements on each of them. The last step in SHM process is to detect the initiation of punching shear cracks and highly stressed compressive spots that exist near the column head. The presence of shear cracks is a warning sign that the applied loads are nearing the ultimate punching shear load. The initiation of shear cracks could be detected using a three-dimensional configuration of FBG sensor arrays (Fig. 4).

### 7 Cyclic load test (CLT) method

The CLT method [23, 24] is used by applying the hydraulic actuators in a stepped loading pattern that is made up of at least three load-sets. Each loading sequence is made up of two or more identical load cycles. The use of identical load cycles within a loading sequence allows for the evaluation of permanency and repeatability. The stepped loading pattern, created by the load increases, allows for the evaluation of deviation from linearity.

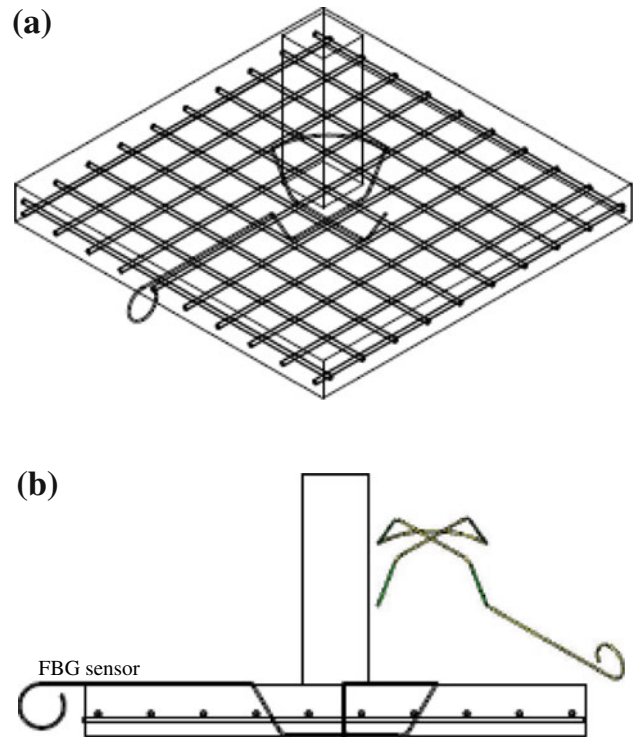


**Fig. 4** Schematic of FBG sensors arrays to detect shear cracks: **a** isometric view, **b** front view

The first load-set should not exceed the service load level or 50% of the expected total test load. The loads are reached in five steps with holds after each step and a hold

at the peak load. Unloading is carried out in the reverse fashion with identical steps and holds. The second load-set is conducted in a similar fashion to the first load-set with a maximum load approximately midway between the initial load-set and the total test load. The final load-set is carried out in the same manner to the total test load. Additional load-sets can be added to the test program. A minimum load  $P_{\min}$  of at least 10% of the total test load should be maintained during each unloading phase to leave test devices engaged. Prior to loading and following the last load-set, the load should be maintained at the benchmark load for initial and final readings.

## 8 Experimental investigation

### 8.1 Development of long FBG sensor

In the current research, a long FBG sensor with a gauge length equal to 300 mm was developed and was embedded in a reinforced concrete two-way slab to detect the initiation of first flexural crack that develops within the slab tension side. The length of FBG sensor was chosen to be greater than the bar spacing,  $s$  (255 mm). The location of the sensor was selected so that the sensor would capture the maximum tensile strain. The FBG sensor was installed to cover the two tensile rebars that were located at the middle of the slab to make sure that FBG sensor will intercept the first crack. Careful attention was paid during the concrete placement, in order to protect the long FBG sensor from damage. Based on a calibration test, the wavelength-strain coefficient for the FBG sensor was estimated to be approximately  $0.95 \text{ pm}/\mu\epsilon$ .

### 8.2 Monitoring system

The acquisition system comprised an optic electronic demodulation unit manufactured by Micron-Optics Incorporation, a PC laptop and a digital interface PCMCIA card. The digital interface card facilitated communication between the PC and the demodulation unit. The FBG-SLI demodulation unit interrogated the wavelengths of the light reflected from the Bragg sensors and sent this information to a software application running on the PC. The FBG-SLI unit is based on a fibre-FP tunable filter and can typically obtain pm wavelength resolution. A custom software application (I-MON E-USB 2.0) running under the Lab-View (National Instruments) programming environment on the PC laptop was developed specifically for controlling the demodulation system and for acquiring and saving data from the sensors. Figure 5 shows a scheme of the wavelength monitoring system.

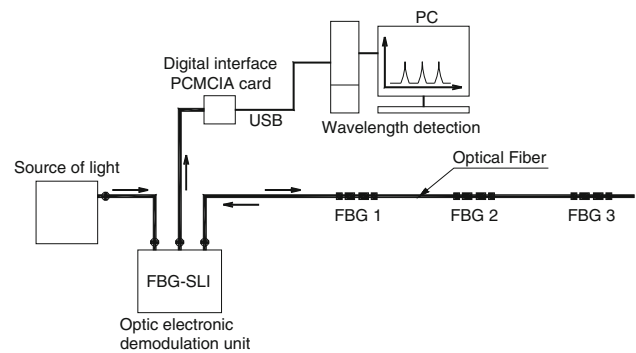


**Fig. 5** Fibre Bragg grating wavelength sensing system

### 8.3 Details of test specimen and instrumentation

The experimental program included testing of a reinforced concrete plate. The test plate had a side dimension of 1,900 mm in both directions. The test plate had a total thickness of 200 mm and an effective depth of 140 mm. Reinforcement ratio of 0.98% was selected for flexural reinforcement. The HSC used in casting the test plate was supplied from a local batch plant. The concrete had a nominal compressive strength of 70 MPa after 28 days. Reinforcing bars consisted of grade 400 steel, conforming to CSA standards with actual tested yield strength of 440 MPa, and yield strain of about  $2,260 \mu\epsilon$ . The test specimen was simply supported along all four edges with the corners free to lift. A concentric load was applied on the plate through a  $250 \times 250$  mm column stub. Two sets of FBG and ESG strain sensors were bonded onto tensile reinforcement (Fig. 6a). A 20-mm gauge length FBG sensor was bonded onto a flattened surface at the middle of the reinforcement rebar. A different type of long FBG sensor (300 mm gauge length) was embedded in the tension side of the concrete plate (Fig. 6b). The objective was to test the capability of long FBG strain sensors to capture the initiation of first crack within the column (loading) area. Conventional four ESGs were bonded onto flattened surfaces of reinforcement bars, as shown in Fig. 6a. The deflection of the slab was measured during loading by five linear variable differential transducers (LVDTs) at five predetermined locations on the tension surface, as shown in Fig. 6c. The readings from the LVDTs were logged into a data acquisition system.

### 8.4 Test procedure

The plate was tested in a vertical position in order to detect and mark the cracks as they developed. The load was applied to the plate concentrically through the stub column. Rubber packing pieces were provided immediately under the plate surface to ensure uniform contact along the

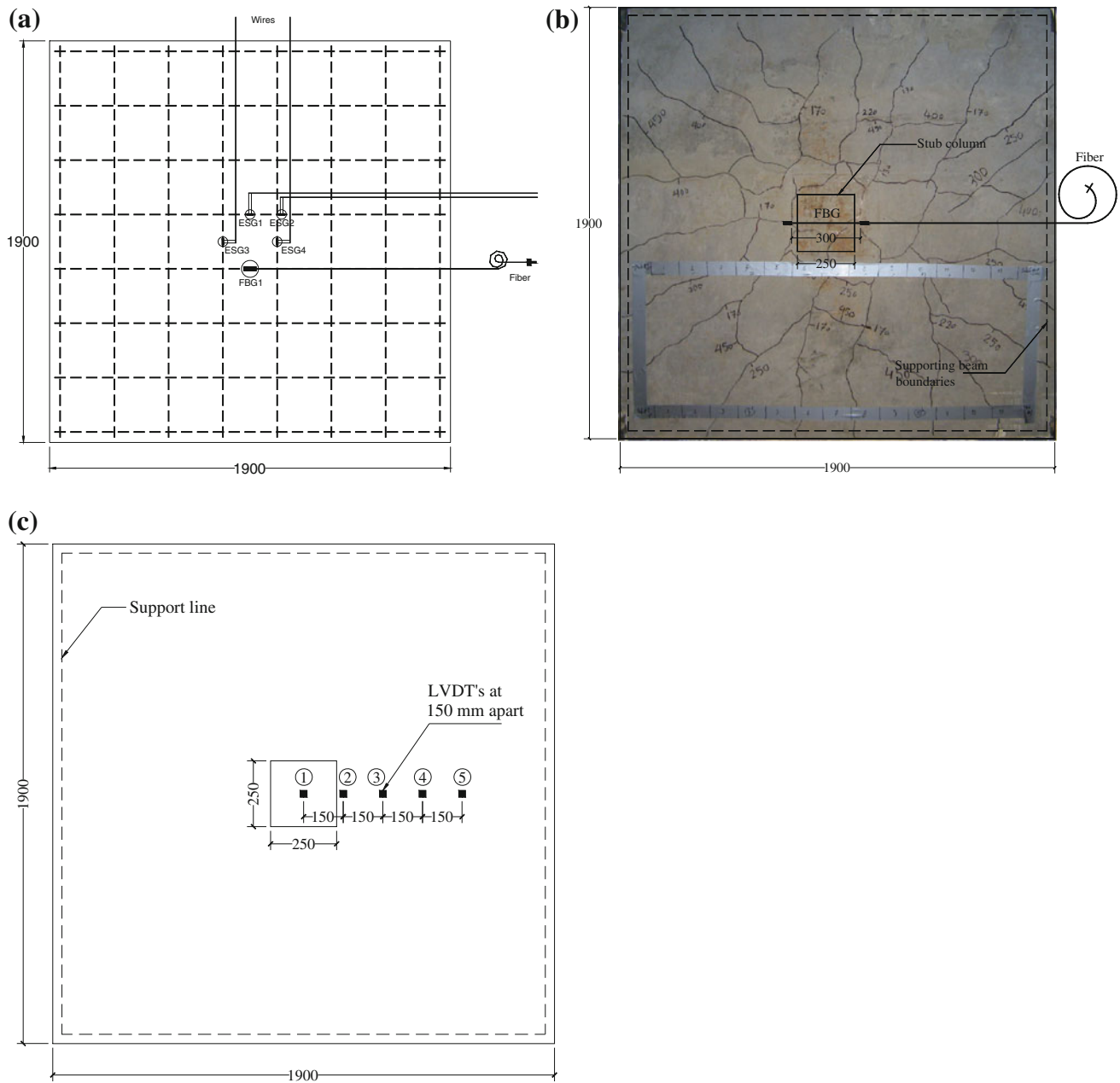


**Fig. 6** FBG and ESG sensors. **a** Sensors bonded onto tensile reinforcement, **b** long FBG sensor embedded in the concrete plate, and **c** arrangement of LVDTs

supports. The test was carried out using a closed-loop (MTS) testing machine with a maximum capacity of 670 kN in load control mode. The load was applied by means of a hydraulic actuator. During testing, the plate was carefully inspected and cracks were marked at each load increment. The loading process involved a cycle test (serviceability limit state test). In the cycle test, a relatively small force was imposed on the plate of approximately

222 kN and then it was released after finishing the test. In this test, the concrete plate was loaded in three load-sets according to the CLT method, as shown in Fig. 7, each load-set was repeated four times to allow enough time for monitoring and marking flexural cracks as they developed. The deformation experienced by the concrete plate was considered as elastic/linear. The maximum loading on the plate for it to be considered elastic is related to 50% of the



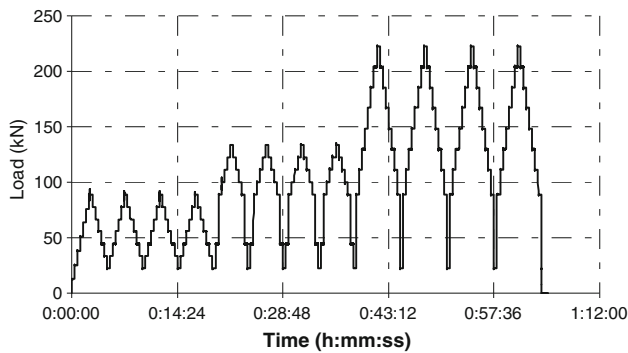


**Fig. 7** Loading profile for service loading test

steel reinforcement yield stress. The magnitude of the first load-set was chosen to represent 40% of service load level. Based on the loading configuration, this corresponded to a total applied load of 90 kN. The last load-set was up to 222 kN and it represented a value less than 50% of the ultimate failure load.

## 9 Test results

### 9.1 Concrete tensile strains

Concrete tensile strains were recorded using an embedded long FBG strain sensor with a gauge length equal to 300 mm. Figure 8 shows the concrete tensile strain versus time curve. In general, the concrete strains indicated that as the load increased, the concrete tensile strain increased gradually up to the initiation of first crack. Flexural cracks begin to occur when concrete stress in the tension face of a member reaches the flexural strength of concrete. After formation of a crack some elastic recovery takes place in concrete on the member surface, contributing to the crack width. The long FBG sensor was able to capture the initiation of the first and second transverse flexural cracks; this is indicated by a sudden increase (shift) in the concrete tensile strain value.

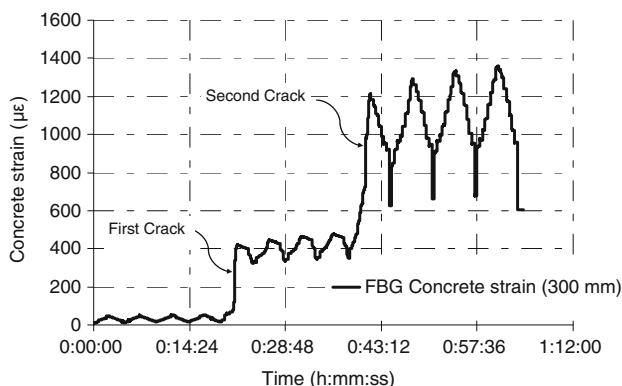


**Fig. 8** Concrete tensile strain versus time (plate test)

For the test slab, the initial observed crack was first formed tangentially under the edge of the column stub, followed by radial cracking extending from the column edge towards the edge of the slab. The first crack occurred at a load equal to 111 kN that represented 16% of the flexural failure load. The first crack width could be calculated by multiplying the difference in the concrete tensile strain ( $340 \mu\epsilon$ ) by the gauge length value (300 mm), and it is equal to 0.102 mm. The same procedure could be used to calculate the width of the second crack as well. The crack pattern observed prior to punching consisted of almost no tangential crack, radial cracking extending from the column was the most dominant crack pattern.

### 9.2 Steel strains

Figure 9a shows a typical load versus steel strain behaviour for all load-sets before and after crack initiation. For the test slab, the tension reinforcement yielded before punching occurred. The yielding of flexural reinforcement occurred at a load that represented 54% of the punching load. Figure 9b shows the comparison between the tensile steel strains obtained using ESG and FBG sensors, under repeated cyclic loading conditions. Obviously, the structural response can be calculated according to the strain measurements shown in Fig. 9a, b. The measured steel strains using FBG sensor (20 mm) are higher than the measured steel strains using ESG sensor (10 mm). The FBG sensor installed on the tensile rebar was working well as expected, and it did not show any significant reduction of sensing performance. However, two of the ESGs installed in the same location of the FBG sensor failed to operate after the strain reached a certain value of  $4,000 \mu\epsilon$ . In this aspect, the FBG sensors demonstrated distinct advantage for long-term health monitoring of concrete structures because of their reliability, durability and accuracy.

### 9.3 Load–deflection and cracking characteristics

The applied load versus the deflection at the centre of the plate for the test plate is shown in Fig. 10. The first yielding of the bottom reinforcement is indicated by a circle on each curve. In general, the slope of the load–deflection curve was normally steep up to failure. It should be noted that the load–deflection curves can be used in classifying failure type. The load–deflection curve indicated that the plate failed in ductile punching, and the load deflection curve was somewhat smooth before failure. However, failure of slab was characterized by a sudden drop in the load–deflection curve. Figure 10 shows also a comparison between the load–central deflection curves for the test slab with another similar slab loaded using

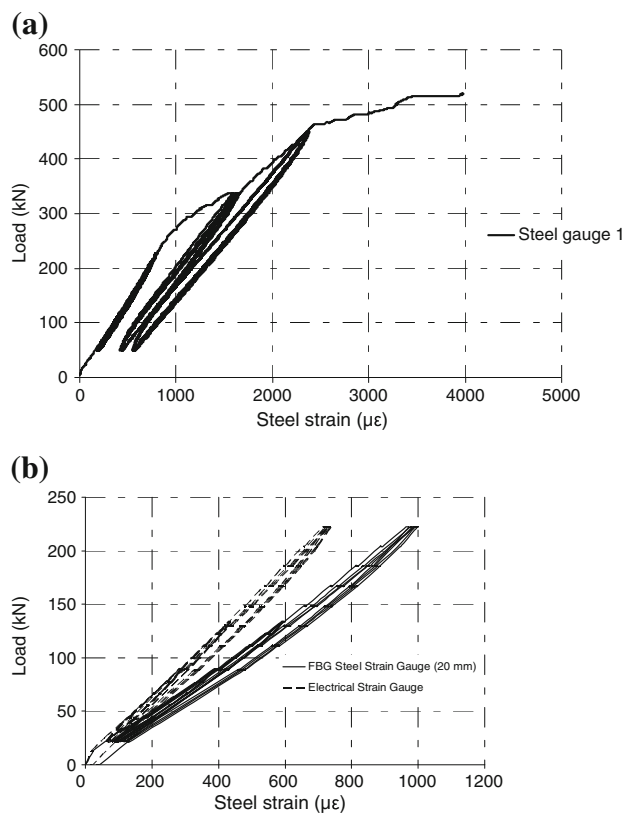


**Fig. 9** Load versus strain for plate test: **a** typical behaviour, **b** strain response of cracked plate under cyclic loading

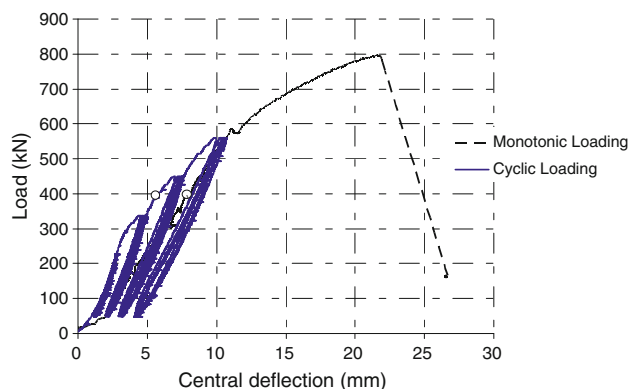


**Fig. 10** Load-central deflection for monotonic and cyclic loading

monotonic loading. It is clear that both monotonic and cyclic load deflection curves had almost the same trend. From the test observations, flexural cracking occurred first, and it advanced roughly from the column outlines towards the plate edges parallel to flexural reinforcement. Subsequently, tangential cracks developed around the vicinity of the column outline. The slab failed at punching load equal to 798 kN, and the failure is characterized as ductile punching.

## 10 Summary and conclusions

The presented work describes a structural health monitoring technique to detect, localize and quantify damage for offshore concrete plates. The experimental program is focused on detection of service (flexural) cracks using embedded long FBG sensors. Detection of flexural cracks includes the initiation of first crack as well as the initial crack width. In the current research, both ESG and FBG sensors were used to monitor tensile strains. Long FBG sensor embedded in concrete slab was successfully used to detect the width and location of the first crack. The FBG sensor was embedded in concrete and was able to survive concrete placement challenges of the construction site thanks to gentle and careful handling. The results show that FBG strain sensor is an effective sensing method in SHM systems for offshore concrete plate structures.

In order to obtain the accurate locations of sensor's monitoring points, a rational STM could be applied. The length of the FBG sensor was chosen to cover at least one bar spacing. The maximum bar spacing could be obtained by applying the formula proposed by Frosch [21] that was implemented later in the recent ACI 318-05 code [22] to control crack through bar spacing limitation.

A new technique is proposed, based on previous research work, to detect and map crack patterns for two-way slabs using FBG sensors arrays. Test results revealed that embedded FBG sensors exhibited excellent performance and it was able to monitor the width and location of the first and second flexural cracks. The CLT method of in-place evaluation provides some clear advantages over the common loading methods. The most significant advantage is that it allows for careful, continuous and repeated monitoring of the structural response and the efficiency of the different sensors to loading, and therefore provides improved insight into structural behaviour.

**Acknowledgments** The authors are grateful to the Natural Sciences and Engineering Research Council of Canada (NSERC) and the Petroleum Research Atlantic Canada (PRAC) for providing the funds for the project. Sincere thanks are due to Mr. Matthew Curtis, Mr. Shawn Organ and the Technical Staff of the Structural Engineering Laboratory of Memorial University of Newfoundland for their assistance during the preparation of the specimens and during testing. Sincere thanks are extended to Capital Ready Mix Ltd., Newfoundland, for providing the concrete for this project.

## References

1. Rytter A (1993) Vibration based inspection of civil engineering. PhD Dissertation, University of Aalborg, Denmark
2. Friebele E (1998) Fibre Bragg grating strain sensors: present and future applications in smart structures. *Optics Photon News* 9(8):33–38

3. Ansari F (1998) Fibre optic sensors for construction materials and bridges. Technomic Publishing, Lancaster
4. Mufti A, Tadros G, Jones P (1997) Field assessment of fibre-optic Bragg grating strain sensors in the confederation bridge. *Canadian J of Civil Eng* 24(6):963–966
5. Tennyson R, Mufti A, Rizkalla S, Tadros G, Benmokrane B (2001) Structural health monitoring of innovative bridges in Canada with fibre optic sensors. *Smart Mater Struct* 10(3):560–573
6. Ansari F, Sture S (1992) Nondestructive testing of concrete elements and structures. ASCE, New York
7. Ansari F (2005) Fibre optic health monitoring of civil structures using long gage and acoustic sensors. *Smart Mater Struct* 14(3):S1–S7
8. Glisic B, Inaudi D (2007) Fibre optic methods for structural health monitoring. Wiley, New York
9. Okabe Y, Yashiro S, Kosaka T, Takeda N (2000) Detection of transverse cracks in CFRP composites using embedded fibre Bragg grating sensors. *Smart Mater Struct* 9(6):832–838
10. Lin Y, Chang K, Chern J, Wang L (2004) The health monitoring of a prestressed concrete beam by using fibre Bragg grating sensors. *Smart Mater Struct* 13(4):712–718
11. Silva-Munoz R, Lopez-Anido R (2009) Structural health monitoring of marine composite structural joints using embedded Fibre Bragg grating sensors. *Comp Struct* 89(2):224–234
12. Takeda N, Minakuchi S, Yamauchi I, Hirose Y (2009) Crack detection for foam core sandwich structures using FBG sensors embedded in a crack arrester, vol 33. *Materials Forum*, Institute of Materials Engineering Australasia Ltd, pp 131–135
13. Muttoni A, Schwartz J (1991) Behaviour of beams and punching in slabs without shear reinforcement. *IABSE Colloquium* 62:703–708
14. Tiller R (1995) Strut-and-tie model for punching shear of concrete slabs. MSc thesis, Memorial University of Newfoundland, Canada
15. Marzouk H, Rizk E, Tiller R (2010) Design of shear reinforcement for thick plates using a strut-and-tie model. *Can J Civil Eng* 37(2):181–194
16. Nawy E (1968) Crack control in reinforced concrete structures. *ACI J Proc* 65(10):825–836
17. Nawy E, Blair K (1971) Further studies on flexural crack control in structural slab systems. In: Philleo RE (ed) *Symposium on cracking, deflection and ultimate load of concrete slab systems*, ACI SP-30, vol 30. American Concrete Institute, Farmington Hills, pp 1–42
18. Nawy E (2001) Design for crack control in reinforced and prestressed concrete beams, two-way slabs and circular tanks. In: Barth FG, Frosch R (eds) *Symposium proceedings on design and construction practices to mitigate cracking*, ACI SP-204, vol 204, pp 1–42
19. Hossin M, Marzouk H (2008) Crack spacing for offshore structures. *Canad J Civil Eng* 35(12):1446–1454
20. Rizk E, Marzouk H (2010) A new formula to calculate crack spacing for concrete plates. *ACI Struct J* 107(1):43–52
21. Frosch R (1999) Another look at cracking and crack control in reinforced concrete. *ACI Struct J* 96(3):437–442
22. ACI Committee 318 (2005) Building code requirements for structural concrete (ACI 318-05) and commentary (ACI 318M-05). ACI 318-05
23. ACI Committee 437 (2003) Strength evaluation of existing concrete buildings. ACI 437R-03
24. Liu Z, Ziehl P (2009) Evaluation of reinforced concrete beam specimens with acoustic emission and cyclic load test methods. *ACI Struct J* 106(3):288–299